Renewable Energy 143 (2019) 611–621

Contents lists available at ScienceDirect

Renewable Energy

journal homepage: www.elsevier.com/locate/renene

Wind turbine lifetime extension decision-making based on structural health monitoring

T. Rubert [a, *], G. Zorzi [a], G. Fusiek [b], P. Niewczas [b], D. McMillan [a], J. McAlorum [b], M. Perry [c]

[a] Doctoral Training Centre in Wind and Marine Energy Systems, University of Strathclyde, 204 George Street, G1 1XW, Glasgow, UK
[b] Department of Electronic & Electrical Engineering, University of Strathclyde, 204 George Street, G1 1XW, Glasgow, UK
[c] Department of Civil & Environmental Engineering, University of Strathclyde, Glasgow, G1 1XJ, UK

ARTICLE INFO

Article history:
Received 23 May 2018
Received in revised form
22 April 2019
Accepted 8 May 2019
Available online 13 May 2019

Keywords:
Structural health monitoring
Wind turbine
Lifetime extension
Fatigue analysis
Remaining useful lifetime
Levelised cost of energy

ABSTRACT

In this work, structural health monitoring data is applied to underpin a long-term wind farm lifetime extension strategy. Based on the outcome of the technical analysis, the case for an extended lifetime of 15 years is argued. Having established the lifetime extension strategy, the single wind turbine investigated within a wind farm is subjected to a bespoke economic lifetime extension case study. In this case study, the local wind resource is taken into consideration, paired with central, optimistic, and pessimistic operational cost assumptions. Besides a deterministic approach, a stochastic analysis is carried out based on Monte Carlo simulations of selected scenarios. Findings reveal the economic potential to operate profitably in a subsidy-free environment with a P90 levelised cost of energy of £25.02 if no component replacement is required within the nacelle and £42.53 for a complete replacement of blades, generator, and gearbox.

1. Introduction

As highlighted by Ziegler et al. [1] in Fig. 1, an increasing number of wind turbine generators (WTG) are reaching their end of design life. For this growing share of WTGs, a justification for lifetime extension may be based on different operational metrics such as: (i) the site classification, for example a turbine designed for a class II site but operated in a class III, (ii) the level of downtime, (iii) the lifetime energy production, (iv) sufficient design reserves, (v) if components are replaced during the design lifetime, and (vi) any combination of the above.

The main advantages of lifetime extension are: (i) the ability to increase the return on investment, with significantly less resources than required in repowering scenarios, (ii) utilise assets until the end of life cycle, thus preventing premature dismantling as well as (iii) using readily available local infrastructure (grid connection, access routes, community ties).

It has been proposed that structural health monitoring (SHM) may play an important role in supporting the process of lifetime extension (LTE) decision-making in order to reduce uncertainty of a turbine's site specific loading or if components are considered critical based on inspections [1–3].

Therefore, this paper applies SHM data from an operational wind turbine to develop an LTE strategy. Subsequently, the proposed strategy is considered jointly with operational data and subjected to an economic decision-making methodology developed by Rubert et al. [4,5]. In order to consider uncertainties in the bespoke wind turbine economic model, uncertainty bands are applied in cost and mean annual energy production. In addition a Monte Carlo simulation is carried out for selected scenarios.

The remainder of this paper is structured as follows. Section 2 compares SHM activities with other forms of analysis to support the lifetime extension decision-making, presents a review of wind turbine tower and foundation SHM research, and the results from the SHM measurement campaign. Section 3 presents the applied LTE decision-making methodology whilst in Section 4, the case study is presented where a strategy is derived and economic input parameters presented. Results of the case study are presented in Section 5, followed by a discussion of the key findings in Section 6. Finally, conclusions outlining key findings are presented in Section 7.

2. SHM for lifetime extension

Lifetime extension decision-making can be based on (i) data

* Corresponding author.
E-mail address: tim.rubert@strath.ac.uk (T. Rubert).

https://doi.org/10.1016/j.renene.2019.05.034
0960-1481/

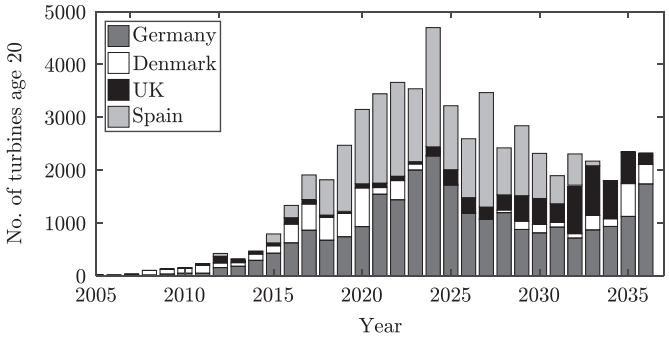

Fig. 1. Turbines reaching end of design life by year [1].

analysis, (ii) inspections, (iii) aero-elastic simulations, and (iv) gathered data through SHM systems. Inspections generate an in-depth assessment of structure's early failure indicators. However, inspections are only valid for a certain period. As such, frequent assessment is necessary in either 3-12 months intervals, thus lacking the ability to support the long-term business case evaluation. Data analysis using SCADA is observed with caution, as the information is often lacking temporally detailed operational history. Aero-elastic simulations may generate a detailed analysis; however, simulations require operational data that might have significant uncertainties, if e.g., taken from SCADA data. Additionally, aero-elastic simulations are generally costly to carry out.

SHM concepts have the ability to provide long-term and in-depth data that can be applied to generate the long-term business case, while delivering a reduced uncertainty in the evaluation.

2.1. Literature review of SHM concepts for wind turbine towers and foundations

With regards to tower sensor installation and data assessment practices, the reader is referred to Smarsly et al. [6] for a 500 kW wind turbine, Rebelo et al. [7,8] for a 2.1 MW wind turbine, Loraux and Brühwiler [9] for a 2 MW wind turbine, and Botz et al. [10] for a 3 MW hybrid turbine consisting of a concrete and steel tower section. The 2 MW wind turbine tower fatigue analysis results in a remaining useful lifetime (RUL) of 135 years in a low mean wind speed region (5.9 m/s) [9].

Related SHM concepts of onshore wind turbine foundations are available by Currie et al. [11,12] aimed at monitoring the displacement between the tower and foundation. Based upon this work, Bai et al. [13] evaluate sensors embedded in concrete blocks, to monitor the displacement and crack development at the bottom of the inserted can flange that area is prone to failure initiation. In this project, empty steel tubes are further vertically inserted in the foundation, facilitating horizontal ultrasonic testing, to identify the structural integrity with height. In addition, Perry et al. [14] and McAlorum et al. [15] present a short and long term crack monitoring solution of wind turbine foundations, whereas Rubert et al. [16] demonstrate a field case study of embedding optical strain gauges in reinforced concrete foundations.

The interested reader is referred to Refs. [17–19] for a general review of SHM opportunities, failures, and inspection practices of wind turbines.

2.2. SHM campaign

The WTG of focus is a multi-MW, individual pitch regulated, onshore generator located in Scotland. Due to confidentiality reasons, the type, manufacturer, and rated power are not disclosed. In addition, all presented data is normalised or the axis labels and tics are removed. The overall SHM installation process, characterisation, temperature compensation, and validation is detailed in Ref. [20]. In comparison to other tower RUL assessments, in this work, a turbine with a greater mean wind speed ($>$ 7 m/s) and greater rated power ($>$ 3 MW) undergoes a load measurement campaign using optical strain gauges at the tower base sampled at a high frequency ($>$ 50 Hz). The overall procedure of the fatigue analysis is taken from available and previously mentioned publications; however, the novelty is to apply SHM information to derive and evaluate the long-term strategic LTE business case for a specific wind farm.

2.2.1. Tower SHM

Ideally, strain gauges are installed at the locations on the tower situated in the prevailing wind direction. However, the installation of tower sensors might not be feasible in all areas; access restrictions and risk of damage due to maintenance processes can limit the available positioning of sensors (e.g. in proximity to the foundation-tower bolts that require servicing). Such constraints were encountered in this work; however, as explored below, the problem of imperfect positioning of sensors has not been of serious consequence to the adopted methodology.

The locations of the tower base strain gauges (T1–T4) with respect to north is illustrated in Fig. 2. The normalised strain data, paired with 30 min average supervisory control and data acquisition (SCADA) wind speed data (in the respective directional corridor ± 10°) is illustrated in Fig. 3 for T1 and in Fig. 4 for the 90° rotated tower strain T2, respectively. Overall, the measurements are well in agreement with the yaw reference SCADA data, allowing confidence in the nacelle sensor calibration.

Based on the measurement campaign, as expected due to access constraints, the sensors are not aligned with the prevailing wind direction. This was confirmed (i) based on the mean SCADA nacelle direction and (ii) since the operational SCADA period of $T1$'s inflow corridor (± 10°) over the total recorded time covered 7.5% and 3.2% for T2, respectively.

In order to evaluate a component's total lifetime based on measured or simulated data, the recorded signal is decomposed in defined discrete cycle ranges and each range's total number of occurrence is counted through a process referred to as rainflow

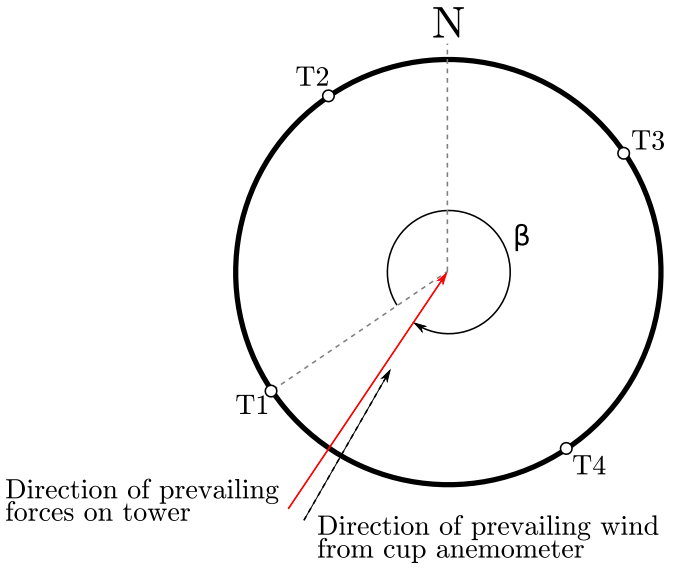

Fig. 2. Schematic of tower sensor positions with respect to prevailing wind direction.

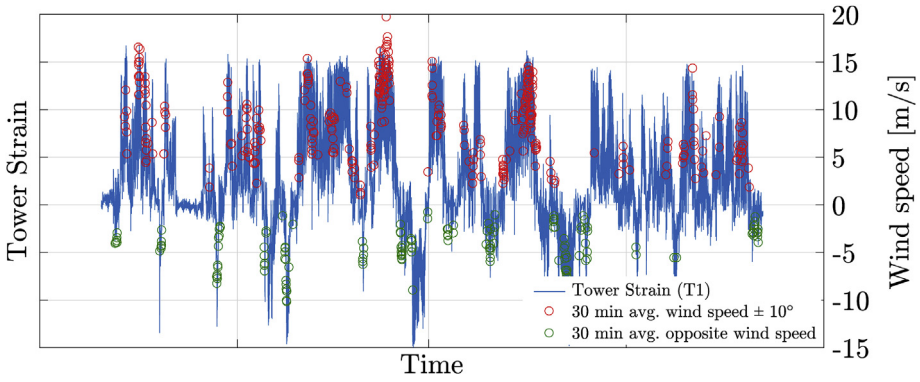

Fig. 3. Strain data of base tower measurement (T1). The data is paired with recorded SCADA wind speed measurements on the right y-axis.

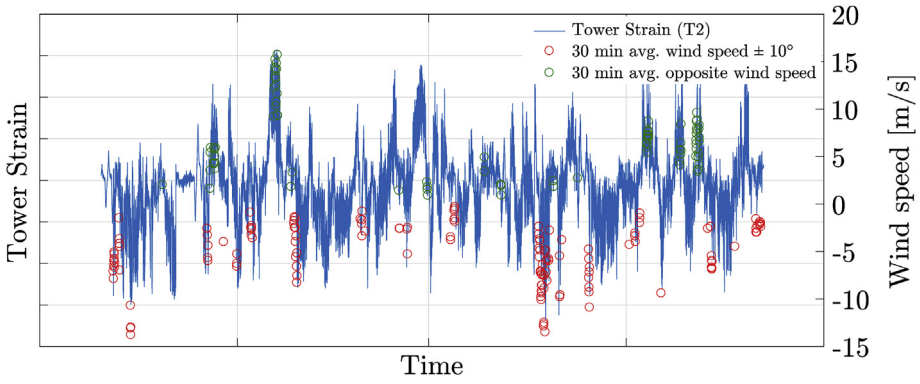

Fig. 4. Strain data of 90° rotated base tower measurement (T2). The data is paired with recorded SCADA wind speed measurements on the right y-axis.

counting [21]. Since, the rainflow counting algorithm is highly sensitive to changes in the maximum strain as well as in the frequency of occurrence of each range [9], the actual prevailing wind direction requires evaluation.

Given that the tower is radially symmetrical and the component's material (S355 steel) is designed to operate in its elastic limit, the stress across the circumference of the tower can be found as a vector sum of the stresses from the sensors. The two sensor strain measurements $v_{T1}(t)$ and $v_{T2}(t)$ respectively from T1 and T2, being positioned on the tower at 90° from each other, allows calculation of the magnitude of the resulting vector, $|v(t)|$, and angle, $\gamma(t)$, by:

$$\left|v(t)\right| = \sqrt{v_{T1}(t)^2 + v_{T2}(t)^2} \tag{1}$$

$$\gamma(t) = \tan^{-1}\left(\frac{v_{T1}(t)}{v_{T2}(t)}\right) \tag{2}$$

The direction of the prevailing forces on the tower (which in turn is dictated by the prevailing wind direction), is identified counting the number of occurrences in the angle $\gamma(t)$ using a moving window of 5° as illustrated in Fig. 5. The prevailing wind direction β with respect to T1 is then identified as the angle with the maximum number of occurrences.

Fig. 5 indicates that the actual prevailing wind direction does not coincide with any sensor positions as it is not a multiple of 90°. In fact, the actual prevailing wind direction is shifted by 22° counterclockwise with respect to T1, which is also closely in agreement with the nacelle's mean SCADA direction with a difference of 3° as illustrated in Fig. 2.

Further, it is necessary to determine if the strain is positive or negative for the rainflow counting as the range (tension and compression) dictates fatigue cycles. Therefore, the difference between angles is calculated:

$$\alpha(t) = \beta - \gamma(t) \tag{3}$$

and the strain variation over time in the prevailing wind direction, denoted as $A(t)$ is calculated by:

$$A(t) = cos(\alpha(t)) \cdot |v(t)| \tag{4}$$

And for the perpendicular direction as:

$$B(t) = sin(\alpha(t)) \cdot |v(t)| \tag{5}$$

It was further verified that of this new set of axes, the higher frequented component is selected.

Fig. 6 displays the calculated strain in the prevailing wind direction. The strain profile is in agreement with the wind speed measurements from the SCADA data. Also, the SCADA data shows that, in the directional corridor considered, the turbine was operational for 23% of the total recorded time. This corroborates the above analysis.

The tower is usually made from hot-rolled steel, welded together circumferentially and longitudinally [22], with welded flanges at either tower end. As such the S-N curve assumption is dependent on the weld type [23]. The rainflow counting algorithm was applied according to the ASTM standard where half cycles are conservatively treated as full cycles [21,24]. The S–N curve for the tower is used with the following parameters. The endurance limit at 2 million cycles, $\Delta\sigma_C = 80$ MPa [23,25], the constant amplitude fatigue limit at 5 million cycles, $\Delta\sigma_D = 59$ MPa, and the cut-off limit,

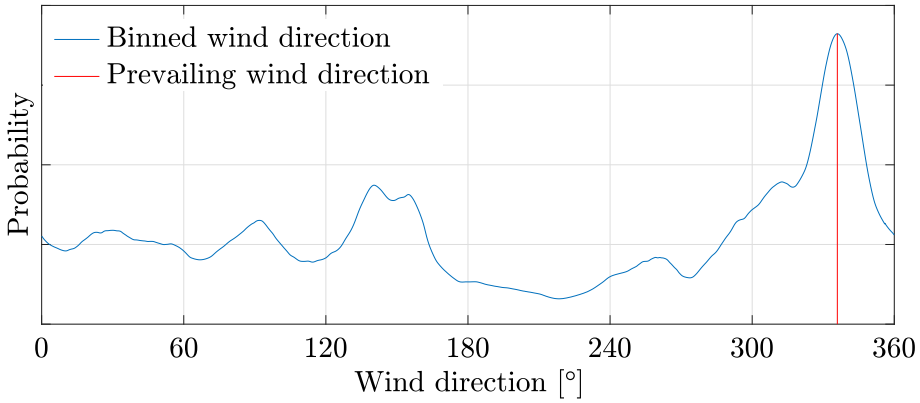

Fig. 5. Identification of prevailing wind direction, β based on $\gamma(t)$ binning. The data is derived from tower strain sensor T1 & T2.

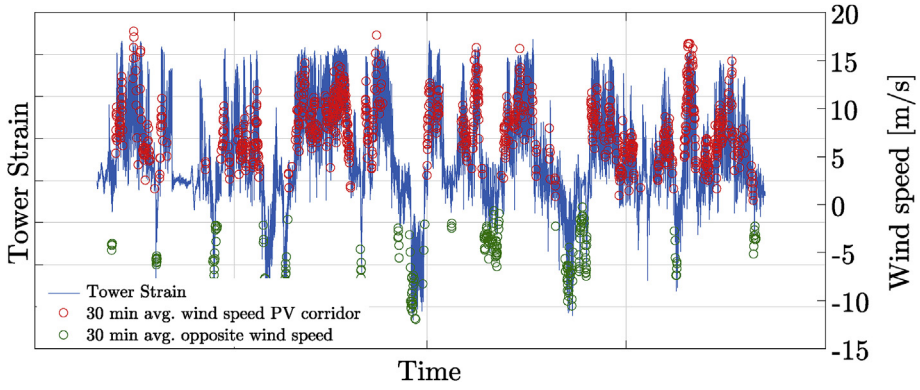

Fig. 6. Strain data of derived prevailing wind direction. The data is paired with recorded SCADA wind speed measurements on the right y-axis.

$\Delta\sigma_L = 32$ MPa according to EN 1993–1–9 [23]. With the established S–N curve, Miner's damage calculation was applied, after the strain was transformed into a stress (Young's Modulus, $E = 200$ GPa). The cumulative fatigue damage D_{tot} is:

$$D_{tot} = \sum D_i \tag{6}$$

where D_i is the partial damage in each discretised rainflow counting bin i. D_i is:

$$D_i = S_m^{-m} \sum_i^N n_i \sigma_i^m \tag{7}$$

where S_m as well as m are material constants, and σ the stress amplitude with n numbers of observed occurrences for the respective bin i. If $\Delta\sigma_i > \Delta\sigma_D$, $m = 3$ and if $\Delta\sigma_L < \Delta\sigma_i < \Delta\sigma_D$, $m = 5$. Otherwise, $D_i = 0$. The total fatigue damage D_{tot} is thus calculated. The binning width of the rainflow counting algorithm and sampling frequency determine the accuracy of the lifetime prediction; however, a high sampling frequency in combination with a small binning width, significantly increase processing requirements. As such, the appropriate binning width of 0.2 MPa was identified as illustrated in Fig. 7 while an appropriate minimum sampling frequency is identified as 100 times the first tower mode as illustrated in Fig. 8.

The total tower lifetime, based on the recorded measurement data $T1$ was thus estimated to be 248 years and for $T2$ 339 years, respectively. In the prevailing wind direction, the derived and more frequented corridor β, the lifetime analysis resulted in a reduced lifetime of roughly 23 years with a total of 225 years.[1] The magnitude of this reduction further allowed confidence in the data processing. In order to verify this result, the lifetime analysis was carried out for varying β (0–180°) as more significant loading, albeit with an overall lower number of occurrence, could have been experienced for wind directions off the prevailing axis. This analysis verified the prevailing wind direction β, identified in Fig. 5.

Further, based on findings by Rebelo et al. [7,8] and Loraux and Brühwiler [26], the maximum tower stress is likely to be experienced at 30–40% of the hub height. At present, the complete tower geometry of the considered wind turbine is unknown. Therefore, a conservatively selected correction factor, derived from the previously mentioned tower monitoring campaigns, is introduced. The corrected total lifetime at the critical tower height is thus identified as 81.6 years. A further correction is required as the outer shell of the tower has a greater stress, as the inner walls' strains are monitored. Thus, this correction leads to a total lifetime of 78.4 years. So far, the carried out stress correction procedure has neglected any reliability aspects. In order to allow for sufficient safety margins, the IEC power production safety factor (1.25) is further applied. With the safety factor included, the total lifetime results in 34.6 years. The overall data processing steps are summarised in Table 1. If residual cycles of the rainflow counting process are treated as half cycles, as suggested by the IEC 61400-13 standard [27], the total lifetime is identified as 35.2 years.

Overall, from the point of view of the tower, a LTE of 15 years

[1] binning width of 0.2 MPa and frequency of 380 times the first tower mode.

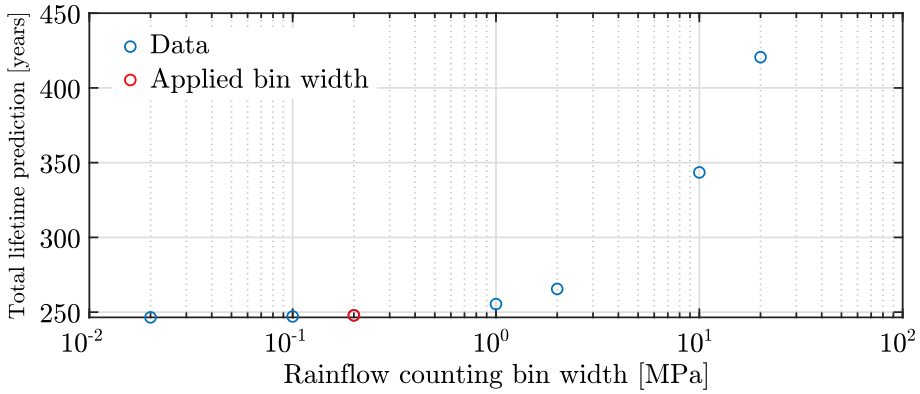

Fig. 7. Impact of binning width on lifetime prediction. Applied frequency is 380 times the first tower mode.

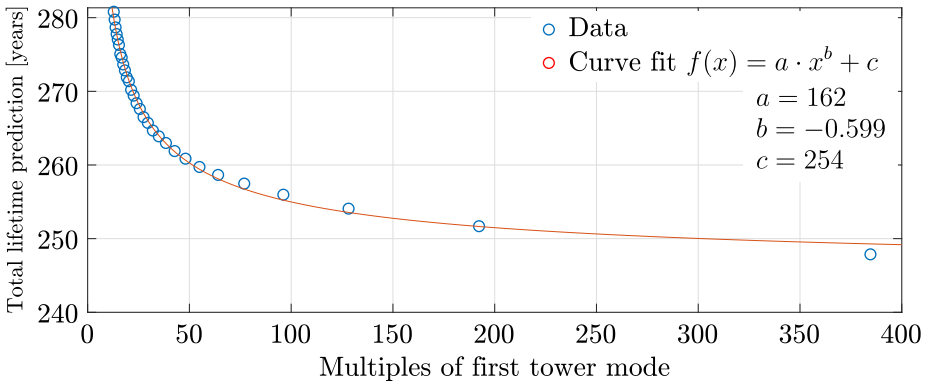

Fig. 8. Impact of sampling frequency on lifetime prediction based on a 0.2 MPa binning width.

thus appears feasible, given considerate safety margin, as the carried out fatigue analysis reveals a total lifetime of 35 years (turbine design life is 20 years).

2.2.2. Foundation SHM

Overall, SHM of wind turbine foundations is a challenging area of research as highlighted by several studies, since the foundation is mainly inaccessible for inspection [13,14,20]. Given that wind turbine foundations (i) are designed for a lifetime of 50 years or more, (ii) their design is based on conservative assumptions, and (iii) they are structurally of key importance, there is little concern to accommodate for LTE. Based on an internal strain analysis of the reinforcement cage by Rubert et al. [20], this is further supported. As a consequence, from an economic lifetime extension decision-making perspective, the foundation is not of concern (except when severe cracks are encountered). "Cracking is normal in reinforced concrete structures subject to bending, shear, torsion or tension resulting from either direct loading or restraint or imposed deformations" [28]. Although cracking is expected to some degree, there is a crack width limit, w_{max} that is governed under the service limit state. The acceptable crack width is dependent on the concrete exposure class and type of reinforcement and can be looked up in design codes and guidelines. Also, if cracks appear, work by Perry et al. [14] and McAlorum et al. [15] may be applied for SHM. Results thus reveal a possibility of an extended WTG operation of greater than 15 years.

Table 1
Process of data manipulation. PW: prevailing wind, HC: height correction, SC: section correction, SF: safety margin. Frequency of 380 times the first tower mode.

Analysis	RUL [years]	Comment
T1 (tower base)	248	Sensor 22° to prevailing wind
T2 (tower base)	339	Sensor 112° to prevailing wind
PW (tower base)	225	Derived prevailing wind with Equation (4)
PW + HC	81.6	Corrected stress at most critical height
PW + HC + SC	78.4	Corrected for the outer shell
PW + HC + SC + SF	34.6	Added IEC safety margin

3. Lifetime extension methodology

The lifetime extension decision-making methodology is schematically illustrated in Fig. 9, where the lifetime extension period is treated as a separate investment and calculated based upon levelised cost of energy ($LCOE_2$). To calculate $LCOE_2$, the net present value (NPV) of costs is divided by the NPV of the annual energy production (AEP):

$$LCOE_2 = \frac{NPV_{costs}}{NPE} = \frac{C_0 + L_0 + \sum_{n=1}^{T} \frac{F_n + O_n + V_n}{(1+d)^n}}{\sum_{n=1}^{T} \frac{E_n}{(1+d)^n}} \quad (8)$$

where NPE is the net present energy, C_0 the equity capital expenditure of component replacements ($CAPEX_{Replace,E}$), L_0 the lifetime extension capital expenditure ($CAPEX_{LTE}$), n is the period ranging from year 1 after the design lifetime to T the final year of operation (end of extended lifetime), F_n the constant annuity payment of the component replacement's expenditure debt in period n

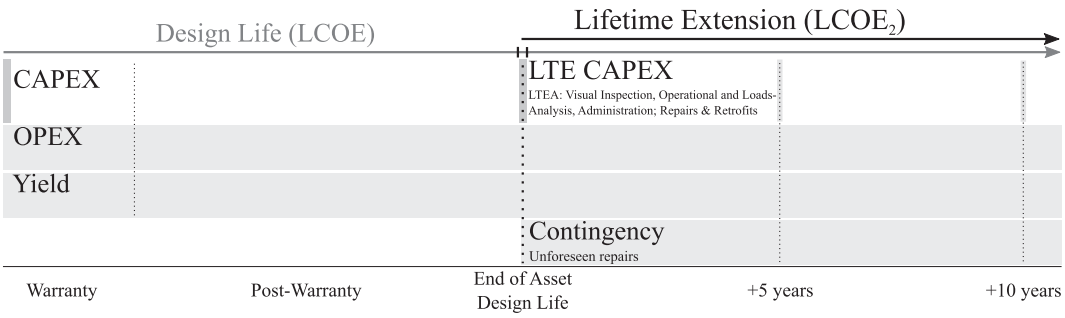

Fig. 9. Lifetime extension decision methodology [4].

($CAPEX_{Replace,D}$), O_n the fixed operating cost including decommissioning[2] in period n, V_n the variable operating cost in period n, E_n the energy generated in period n, and d the discount rate.

This extended lifetime methodology is equipped with operational data in terms of cost and yield parameters. The prior includes the $CAPEX_{LTE}$ and operational & maintenance (O&M) expenditure and the latter identified through operational knowledge or alternatively the application of a Weibull wind distribution in combination with a turbine's power curve [29]. Of course all variables are ideally based upon the operational design lifetime and may be adjusted depending on; e.g., failure and reliability data.

4. Lifetime extension case study

4.1. Strategy

The structural integrity of the foundation and tower is one of the main factors in determining economic lifetime extendibility (high replacement costs) and the high importance in serving as a load-carrying component, their RUL is of significant interest for a given wind turbine. As previously discussed, the foundation design lifetime significantly exceeds other components, provided that the design and construction procedures have been correct. Hence, in the great majority of cases, the tower RUL is of greater concern. Therefore, knowledge of the site-specific tower RUL will provide argument for the long-term economic business case.

The results from the SHM campaign presented above indicate that lifetime extension of 15 years appears feasible. Therefore, for the LTE business case the strategic extension period is considered to be 15 years.

4.2. Input data

The input data for the economic model is a combination of actual and generic data as illustrated in Table 2. Where possible, real input is applied; however, the commercial business case is highly sensitive, thus not all actual data is applied in the model. As such, the economic model generates an academic case scenario that is aligned as best as possible to a potential real scenario. The power curve was reproduced as highlighted by Rubert et al. [4]; however, rather than applying the maximum power coefficient, $C_{p,max}$ to derive the power curve, C_p varies with wind speed, $C_p(v)$ that was derived based on the manufacturer's data sheet ($\rho = 1.225$ Kg/m^3). This enables greater accuracy in the yield modeling as outlined by Carillo et al. [30] and Lydia et al. [31].

As identified by Refs. [4,32], the mean wind speed has the highest magnitude in the impact, thus careful evaluation is necessary. The turbine's mean wind speed was derived using operational SCADA data, accounting for the impact of curtailment (provided by the operator). Curtailment was included in the model by reducing the average wind speed for the specific wind turbine.

Table 2
Wind turbine parameters. Actual are real operational parameters for the respective wind turbine, while generic data is applied due to confidentiality in the business case. The resulting capacity factor is a combination as actual and generic data is applied to derive the metric.

Parameter	Value	Actual/Generic Data
Cut-in wind speed	3 [m/s]	Actual
Cut-out wind speed	25 [m/s]	Actual
Rated wind speed	12.5 [m/s]	Actual
Rotor diameter	Not disclosed	Actual
Wind speed	Not disclosed	Actual
Power coefficient	Not disclosed	Actual
Turbulence intensity	0.1	Generic
Availability	97 [%]	Generic
Wake & park losses	10 [%]	Generic
Discount factor	7.5 [%]	Generic
Inflation	1.5 [%]	Generic
Weibull shape factor	2	Generic
Resulting capacity factor	Not disclosed	Actual/Generic

Given that the foundation and tower are able to facilitate the target lifetime extension period, components along the drive train may require replacement. This is budgeted as $CAPEX_{SPARE,D}$ and $CAPEX_{SPARE,E}$ with a 70/30% debt-equity split, the latter budgeted as a constant annuity with the interest rate set as 3.5% [33]. Cost and time assumptions for the necessary crane (1200 t) and service team for component replacements were evaluated. The time requirement was increased by 50% and the service team number increased by 25% from those from Ref. [4]. The overall cost assumptions are summarised in Table 3 for the central case as well as optimistic and pessimistic scenario, respectively.

The discount factor is assumed at 7.5%, with inflation set at 1.5% accounted to administration and spare parts of the O&M expenditure.[3]

Also, for the scenario with no component replacement, an annual performance degradation of 0.3% is modeled based on findings by Refs. [5,35,36]. In the other scenarios, due to component upgrades the performance degradation is likely significantly smaller and thus neglected.

To get greater confidence limits, a Monte Carlo simulation is further applied based on the application of normal distributions. This allows to account for statistical factors, as component/

[2] onshore it is expected that the scrap value equalises decommissioning costs; offshore this is certainly not the case.

[3] The interested reader is referred to Ref. [34] for detailed commentary on LCOE input parameters.

Table 3
Generic lifetime extension cost estimations for a wind farm [4]. The range interval is applied in the Monte Carlo simulation, with the central parameter defined as the median value.

Parameter	Central	Range	Unit
O&M			
Fixed	30,192	22,644–37,740	£/MW/y
Variable	5.1	3.83–6.38	£/MWh
Insurance	2226	1669–2782	£/MW/y
Connection charges	3810	2857–4762	£/MW/y
CAPEX LTE			
Visual inspection	2689	2017–3361	£/WTG
Loads analysis	3500	2625–4375	£/WTG
Operations analysis	2000	1750–2250	£/WTG
Administration	1000	750-1250	£/WTG
Spare parts			
3 blades	238,560	178,920–298,200	£/WTG
Gearbox	147,680	110,760–184,600	£/WTG
Generator	93,152	69,864–116,440	£/WTG
Installation expenditure			
Crane Mob/Dmob	20,000	15,000–25,000	£/Wind Farm
Crane operation	2000	1500–2500	£/day
Service personal	58	43.1–71.9	£/h

installation costs and the wind inflow parameters may vary over time. As such, variability in the results are expected.[4] This was carried out for the scenario with no component replacement and the exchange of the entire drive train. The annual wind speed was characterised based on SCADA mean data paired with a standard deviation of 7% [39]. The cost data was modeled with a standard deviation of 25% as illustrated in Table 3. For the component replacement process, if the wind speed is above a certain wind speed threshold, components cannot be lifted. Therefore, the required crane and service hours were applied based on the minimum expected time and a normally distributed time component added to account for wind related delays. Based on the procedure detailed by Vose [37], the number of required iterations n was identified as 50,000 based on a standard error of 3% and a 90% confidence interval.

5. Results

When operating a wind farm, each turbine can be characterised differently; i.e., some turbines have greater average wind speeds than others, depending on the local terrain, wake effects, and operational parameters. With regards to LCOE calculations, the mean wind speed has the greatest impact [4,32]. When pairing the mean wind speed with operational knowledge (downtime, degradation, curtailment, etc.) the AEP or capacity factor can be derived. Therefore, when operating a wind farm that is reaching its end of design lifetime with fewer revenues or when directly exposed to the spot-market electricity price, some turbines might be less profitable in their continued operation than others. As a consequence, a LTE decision-making requires turbine specific evaluation.

The lifetime extension $LCOE_2$ of the bespoke economic turbine model based on operational wind conditions are illustrated in Fig. 10 under the assumption of (i) no retrofit and (ii) the exchange of the entire drive train; in Fig. 11 for a single retrofit of a drive train component; and in Fig. 12 for any retrofit combination of drive train components. As mentioned before, each scenario has an assumed extended lifetime of 15 years.

The error bands are based on the cost variation illustrated in Table 3. A wind farm usually consists of several individual turbines,

[4] For detailed information of Monte Carlo simulations, the reader is referred to Refs. [37,38].

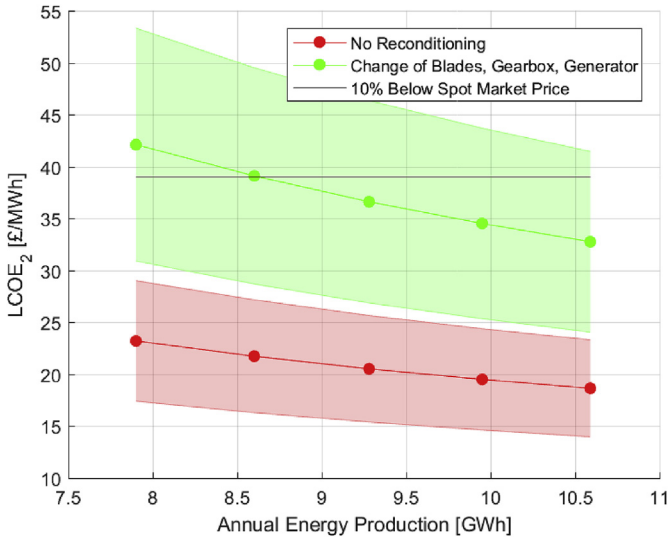

Fig. 10. $LCOE_2$ of lifetime extension period with annual energy production (no retrofitting and drive train exchange).

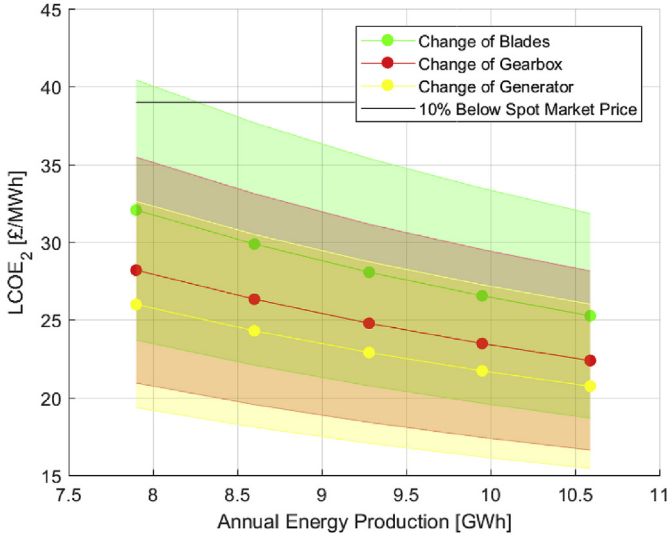

Fig. 11. $LCOE_2$ of lifetime extension period with annual energy production (single retrofit).

with varying degree of loading and electricity production, thus when it comes to lifetime extension, not necessary all turbines are economically suitable to keep in operation. Knowing that the annual wind speed and hence AEP has the greatest impact on LCOE, the wind speed is varied in order to determine profitability of the different cases.

With turbines mostly being exposed to the subsidy-free spot market electricity price, a threshold is defined to determine individual turbine suitability. This is defined as 10% below the average UK's spot market price of the past 5 years [4].

Overall, without any component replacement, the $LCOE_2$ is significantly below the defined subsidy-free threshold (£39), hence LTE is supported for any of the modeled AEP cases. Alternatively, if the entire drive train requires replacement (blades, gearbox, and generator), this would only be economically viable if the annual energy production is above 8.6 GWh/WTG. The complete range is illustrated in Fig. 10.

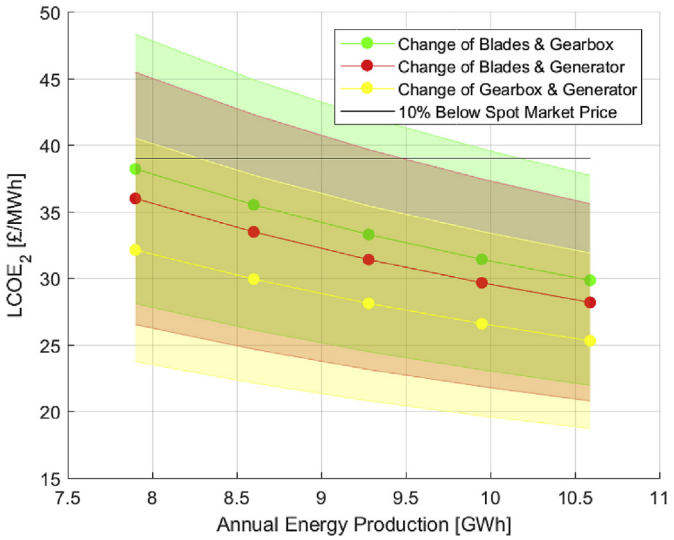

Fig. 12. $LCOE_2$ of lifetime extension period with annual energy production (double retrofit).

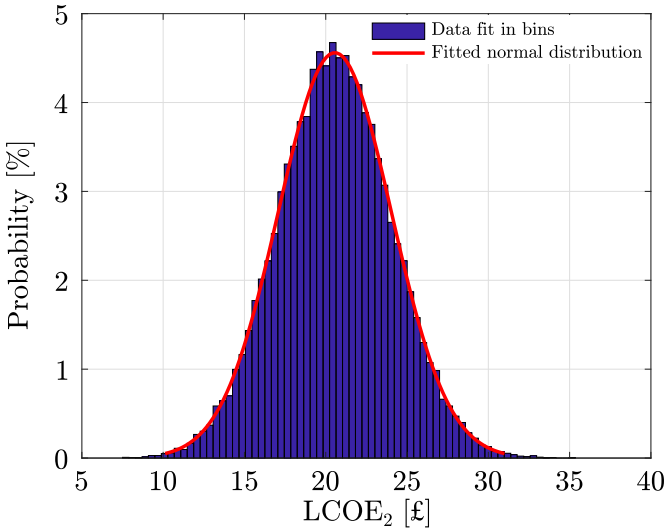

Fig. 13. Monte Carlo analysis of $LCOE_2$ of no component replacement.

For any single component exchange (blades, gearbox, and generator), all medium cost estimates are below the threshold; however, for the pessimistic cost scenario, the replacement of blades are economically infeasible and decommissioning is advised as illustrated in Fig. 11 when below 8.3 GWh/WTG.

For any two component replacement scenario, the cases including new blades require at least 7.5 GWh/WTG when paired with a generator exchange, and 7.8 GWh/WTG when paired with a gearbox exchange in order to be economically viable as illustrated in Fig. 12. The replacement of a gearbox in combination with the generator is feasible in the medium cost scenario; however, in a pessimistic scenario caution is required.

Table 4 further displays the annual available contingency with respect to (i) the different replacement scenarios and (ii) the expenditure range based on an AEP of 9.3 GWh. As illustrated in Fig. 9, this parameter indicates the potential money to spend before the project becomes non-profitable along the life extended period; i.e., when decommissioning is advised. The remaining contingency may be applied to support the operational LTE decision-making as the available budget indicates the risk of an aimed strategic decision. An example would be if the replacement of the drive train is strategically considered matched with central cost estimates, as the remaining annual contingency is £24,980/WTG. In such an event, if severe issues occur (such as a main bearing failure), the project is likely more risky to be profitable than other decisions with a greater annual contingency. This risk can potentially be reduced by in-depth structural analysis and the application of reliability models based on inspection results.

Results of the Monte Carlo simulation are presented in Fig. 13 with no component replacement and in Fig. 14 for the replacement of the entire drive train. In addition, Table 5 presents the respective P10/50/90 percentiles.

Overall, there is a 90% probability that the $LCOE_2$ is below £25.02 with no component replacement, whereas when exchanging the entire drive train, there is a 50% chance that $LCOE_2$ are above £37.07. With respect to the threshold spot market electricity price, there is a 69% chance to be economically profitable. Of course, results of the Monte Carlo simulation will change with differently encountered mean AEP.

6. Discussion and future work

Confidence in the SHM measurement campaign increases as a function of the duration of the data monitoring campaign; a longer monitoring period will thus deliver an increase in confidence in the strategic LTE business case.

Applying the AEP of each turbine requires closer examination as often turbines are curtailed due to network restrictions. Therefore, besides looking at the AEP in isolation, curtailment information can deliver a more accurate picture. Also, when having operated a wind farm for 20 years, its grid integration is well understood and thus data readily available.

As identified by Tavner [40], Wilson [41], and Reder [42], wind turbine reliability is correlated with environmental conditions. Thus, a turbine's components have an individual and thus varying load profile. Of course, the design of the respective turbine should accommodate for such differences given the IEC classes (IEC 61400-1). The turbine in question was identified based on the highest annual wind speed of the respective wind farm. Nevertheless, such

Table 4
Annual contingency [£] for 15 year LTE under different scenarios. N/A: costs exceed revenue.

Scenario	Pessimistic	Central	Optimistic
No reconditioning	141,363	186,268	231,173
Reconditioning of blades	37,704	104,901	173,560
Reconditioning of gearbox	76,837	135,610	195,286
Reconditioning generator	99,283	153,214	207,719
Reconditioning blades, gearbox, & generator	N/A	24,980	116,871
Reconditioning blades & bearbox	N/A	56,138	138,952
Reconditioning blades & generator	N/A	73,743	151,385
Reconditioning gearbox & generator	37,221	104,452	173,158

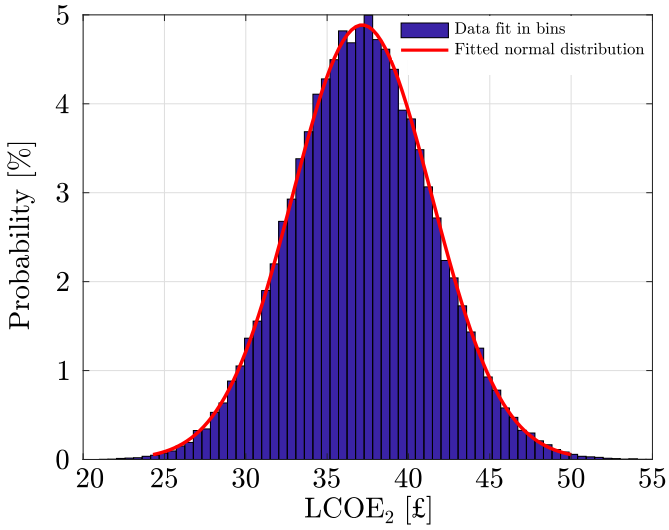

Fig. 14. Monte Carlo analysis of $LCOE_2$ of drive train exchange.

Table 5
Project expenditure percentiles [£] based on Monte Carlo simulation.

Scenario	P10	P50	P90
No replacement	16.10	20.54	25.02
New drive train	31.68	37.07	42.53

indicators as turbulence intensity are also important. The O&M costs may therefore fluctuate per turbine and should ideally be taken into consideration in the economic evaluation. In order to accommodate fluctuations, the optimistic and pessimistic cost bands are presented.

While local wind conditions may change over the years [43,44], so in turn would the AEP. Therefore, when extracting the AEP, a period of several years should be considered. Ideally, the entire operational life.

It is further possible to extrapolate tower fatigue findings onto each individual wind turbine in the wind farm by application of a tower finite element model and, ideally, analysis of high frequency SCADA data (if available). This will be considered in future work, in order to determine a wind farm lifetime extension strategy, by clustering turbines into cells with different loading. In this regard, low wind speed and turbulence intensity exposed wind turbines might be selected for turbine removal and the spare parts might be stored or straight away used to replace turbine components with higher mean wind speed and turbulence intensity values.

Judging from the cost to carry out a tower measurement campaign (roughly £20,000–30,000), we argue that to gain an accurate LTE strategy, the benefit outweighs the costs of the installation of such a system. Of course, the latter depends on the deployed turbine and wind farm size [5] as well as the SHM system design.

We further suggest to install tower sensor sets (one sensor each side for validation purposes [20]) 90° apart as well as to analyse each wind corridor by varying β in order to cover any eventualities if e.g., the assumed prevailing wind direction does not match the real prevailing wind corridor as highlighted in Section 2.2. In addition, as the cross sectional moment of inertia and bending moment change with tower height, so does the stress distribution. Ideally, the tower wall thicknesses and sectional diameters are measured to derive the maximum stress location. Nevertheless, in the absence of tower geometry data, correction factors may be applied as highlighted in Section 2.2. Overall, we strongly recommend to measure the tower's geometry (thickness and diameter with hub height) to identify the most critical stress location. At this location, the fatigue analysis shall be carried out. As such, the application of generic or simplified tower geometries may lead to severe uncertainties and inaccuracies of aero-elastic simulations and thus caution is advised.

The SHM monitoring campaign may be tailored for a global analysis aimed at evaluating stresses of critical tower areas, such as along the entrance door[5] as well as flanges as discussed by Schedat et al. [46].

With respect to the rainflow counting algorithm, we suggest to use a binning width equal or lower than 0.2 MPa paired with a minimum sampling frequency of 100 times the first tower mode. This allows accurate measurements while maintaining an appropriate accuracy (within 10%). Also, a correction parameter can be applied based on the findings presented in Figs. 7 and 8 if data is available at a lower sampling frequency.

SHM data combined with economic findings do not suggest that long-term lifetime extension should be carried out blindly, thus the necessary inspections are key in making sure that the continued operation is safe. For the tower, critical sections are welded and bolted connections as well as areas with corrosion [3,45]. An inspection guideline published by DNV GL for the tower and foundation is presented in Table 6 of the Appendix. In addition, an inspection guideline is published by Megavind [45]. In critical cases, it is further suggested to reduce the inspection interval or to install tailored SHM hardware. For an example of tower flange cracking, the reader is referred to work developed by Do et al. [47]. To access experimental mechanical and fracture properties of welded S355 steel, work by Mehmanparast et al. [48] is suggested. We also recommend monitoring the first natural frequency as well as damping ratio of the tower as variations can indicate structural changes with little resources spend, if sensors are installed.

As illustrated by Helm [49] based on data by the Department for Business, Energy, Industry, and Strategy (BEIS), the electricity price is expected to remain at current prices and then gradually increase from 2020, reaching a high in 2024 before dropping off in the UK. In fact, this requires careful observation and scrutiny in order to define the profitability threshold appropriately.

Uncertainties further origin from the weld assumption; data that is not necessarily shared by turbine manufacturers. Potentially, the weld class might be analysed with ultrasonic wall thickness measurement devices to get confidence in the selection of the appropriate weld classes.

Finally, in comparison to previous findings by Rubert et al. [4], this work derives the strategic lifetime extension case for a significantly greater rated turbine taking the actual structural integrity into consideration as well as the actual wind speed. As such, the lifetime extension business case appears in general more positive than the assessment of smaller scale generators.

7. Conclusion

This work explores a strategic case specific lifetime extension decision-making process, based on information gathered through SHM. The process indicates that if the tower and foundation are in a good condition (acceptable level of corrosion, no cracks for the tower; foundation cracks within acceptable limit), these key

[5] According to the publication from Megavind, the tower entrance door is not considered as a critical area: "As for tower fatigue, cracks in the door-tower connection may, with low probability, occur when the turbine reaches the design lifetime" [45].

turbine components are generally well suited to facilitate lifetime extension decision-making.

Based on the SHM of the wind turbine tower, the total lifetime was identified as 35 years by evaluation of the prevailing wind direction at the most critical tower location, including a load safety margin. In addition, parameters are provided for the analysis to derive the tower's RUL.

Forwarding the structural information to the economic business case, results suggest a P90 $LCOE_2$ of £25 if no components require reconditioning, paired with a lifetime extension of 15 years. If the blades, gearbox, and generator are exchanged in year 20, the P90 $LCOE_2$ is identified as £42.50. For this case, the probability to be 10% below the average spot market price is 69%, thus caution and due diligence is advised or alternatively a lower profit margin shall be defined.

Overall, the results of this study further support the operational knowledge that lifetime extension is highly site specific; however, it is essential to derive a suitable LTE strategy for the continued operation to generate the economic business case. This is especially valid for multi-MW turbines with substantial annual energy production. Besides allowing continued electricity generation and maintaining local O&M jobs, lifetime extension reduces the generation of waste, which is of general interest.

Acknowledgment

This work was funded by Scottish and Southern Energy (SSE), ScottishPower Renewables (SPR) and the EPSRC (Grant No. EP/L016680/1).

Appendix

Table 6
Tower & foundation inspection guideline [3]. D is damage, C is cracks, Co is corrosion, Sp is safety sign plates, Ps is prestress, Cf is connection/fitting, and F is function.

Tower Component	Inspection
Tower structure	D,Co,C,Sp
Ladder, fall protection	D,Co,F,Sp
Bolted connections	Co,Ps,C
Foundation, embedded section	D,Co,C
Foundation	D,C
Grounding/earthing strip	Cf,D,Co

References

[1] L. Ziegler, E. Gonzalez, T. Rubert, U. Smolka, J.J. Melero, Lifetime extension of onshore wind turbines: a review covering Germany, Spain, Denmark, and the UK, 2, Renew. Sustain. Energy Rev. 82 (2018) 1261–1271 [Online]. Available: http://linkinghub.elsevier.com/retrieve/pii/S1364032117313503.

[2] G.L. DNV, Service Specification: Certification of Lifetime Extension of Wind Turbines, 2016 [Online]. Available: https://rules.dnvgl.com/docs/pdf/DNVGL/SE/2016-03/DNVGL-SE-0263.pdf.

[3] Standard: Lifetime Extension of Wind Turbines, 2016 [Online]. Available: https://rules.dnvgl.com/docs/pdf/DNVGL/ST/2016-03/DNVGL-ST-0262.pdf.

[4] T. Rubert, D. McMillan, P. Niewczas, A decision support tool to assist with lifetime extension of wind turbines, Renew. Energy 12 (2018) [Online]. Available: http://linkinghub.elsevier.com/retrieve/pii/S0960148117312685.

[5] The effect of upscaling and performance degradation on onshore wind turbine lifetime extension decision making, 11, J. Phys. Conf. Ser. vol. 926 (2017) 012013 [Online]. Available: http://stacks.iop.org/1742-6596/926/i=1/a=012013?key=crossref.63b19258ed5ed2069d531236b4256c69.

[6] K. Smarsly, D. Hartmann, K.H. Law, An integrated monitoring system for lifecycle management of wind turbines, Int. J. Smart Struct. Syst. 12 (2) (2012) 209–233.

[7] C. Rebelo, M. Veljkovic, L.S. Da Silva, R. Simes, J. Henriques, "Structural monitoring of a wind turbine steel tower - Part I: system description and calibration, Wind Struct. Int. J. 15 (4) (2012) 285–299.

[8] C. Rebelo, M. Veljkovic, R. Matos, L. Simes Da Silva, "Structural monitoring of a wind turbine steel tower - Part II: monitoring results, Wind Struct. Int. J. 15 (4) (2012) 301–311.

[9] C. Loraux, E. Brühwiler, The use of long term monitoring data for the extension of the service duration of existing wind turbine support structures, 9, J. Phys. Conf. Ser. 753 (2016) 072023 [Online]. Available: http://stacks.iop.org/1742-6596/753/i=7/a=072023?key=crossref.bb556abb5450ef12dd546de70c99ecb2.

[10] M. Botz, S. Oberlaender, M. Raith, C.U. Grosse, Monitoring of wind turbine structures with concrete - steel hybrid - tower design, in: 8th European Workshop On Structural Health Monitoring (EWSHM 2016), 2015, pp. 5–8, no. August.

[11] M. Currie, F. Quail, M. Saafi, Development of a robust structural health monitoring system for wind turbine foundations, in: ASME Turbo Expo, 2012. Copenhagen, 2012.

[12] M. Currie, M. Saafi, C. Tachtatzis, F. Quail, Structural integrity monitoring of onshore wind turbine concrete foundations, Renew. Energy 83 (11 2015) 1131–1138 [Online]. Available: http://linkinghub.elsevier.com/retrieve/pii/S0960148115003675.

[13] X. Bai, M. He, R. Ma, D. Huang, Structural condition monitoring of wind turbine foundations, 9, in: Proceedings of the Institution of Civil Engineers - Energy, 2016, pp. 1–19 [Online]. Available: http://www.icevirtuallibrary.com/doi/10.1680/jener.16.00012.

[14] M. Perry, J. McAlorum, G. Fusiek, P. Niewczas, I. McKeeman, T. Rubert, Crack monitoring of operational wind turbine foundations, 8, Sensors 17 (8) (2017) 1925 [Online]. Available: http://www.mdpi.com/1424-8220/17/8/1925.

[15] J. McAlorum, M. Perry, G. Fusiek, P. Niewczas, I. McKeeman, T. Rubert, Deterioration of cracks in onshore wind turbine foundations, Eng. Struct. 167 (7 2018) 121–131 [Online]. Available: http://linkinghub.elsevier.com/retrieve/pii/S0141029617329644.

[16] T. Rubert, M. Perry, G. Fusiek, J. McAlorum, P. Niewczas, A. Brotherston, D. McCallum, Field demonstration of real-time wind turbine foundation strain monitoring, 12, Sensors 18 (2) (2017) 97 [Online]. Available: http://www.mdpi.com/1424-8220/18/1/97.

[17] N. Beganovic, D. Söffker, Structural health management utilization for lifetime prognosis and advanced control strategy deployment of wind turbines: an overview and outlook concerning actual methods, tools, and obtained results, Renew. Sustain. Energy Rev. 64 (10 2016) 68–83 [Online]. Available: http://linkinghub.elsevier.com/retrieve/pii/S1364032116301952.

[18] M. Luengo, A. Kolios, Failure mode identification and end of life scenarios of offshore wind turbines: a review, Energies 8 (8) (2015) 8339–8354 [Online]. Available: http://www.mdpi.com/1996-1073/8/8/8339/.

[19] M.L. Wymore, J.E. Van Dam, H. Ceylan, D. Qiao, A survey of health monitoring systems for wind turbines, Renew. Sustain. Energy Rev. 52 (12 2015) 976–990 [Online]. Available: http://linkinghub.elsevier.com/retrieve/pii/S1364032115007571.

[20] T. Rubert, M. Perry, G. Fusiek, J. McAlorum, P. Niewczas, A. Brotherston, D. McCallum, Field demonstration of real-time wind turbine foundation strain monitoring, Sensors 18 (1) (12 2017) 97 [Online]. Available: http://www.mdpi.com/1424-8220/18/1/97.

[21] H.J. Sutherland, On the Fatigue Analysis of Wind Turbines, Albuquerque, New Mexico, 1999.

[22] N. Stavridou, E. Efthymiou, C.C. Baniotopoulos, Welded connections of wind turbine towers under fatigue loading: finite element analysis and comparative study, Am. J. Eng. Appl. Sci. 8 (4) (2015) 489–503.

[23] European Union, EN 1993-1-9 (2005): Eurocode 3: Design of Steel Structures - Part 1-9: Fatigue, 2005 [Online]. Available: http://www.phd.eng.br/wp-content/uploads/2015/12/en.1993.1.9.2005-1.pdf.

[24] ASTM, Standard practices for cycle counting in fatigue analysis. Standard E1049-85, 2011.

[25] F. Lueddecke, Tower Flange Weld Assumption, 2018.

[26] C. Loraux, Long-term Monitoring of Existing Wind Turbine Towers and Fatigue Perfromance of UHPFCR under Compressive Stresses, 2018 [Online]. Available: https://infoscience.epfl.ch/record/234540.

[27] IEC, 61400-13 2001, 2003, pp. 0–4.

[28] European Union, BS EN 1992-1-1:2004 - eurocode 2: design of concrete structures - Part 1-1: general rules and rules for buildings, Tech. Rep. (2004) [Online]. Available: https://law.resource.org/pub/eu/eurocode/en.1992.1.1.2004.pdf.

[29] T. Burton, N. Jenkins, D. Sharpe, E. Bossanyi, Wind Energy Handbook, John Wiley and Sons, Ltd, Chichester, UK, 5 2011 [Online]. Available: http://doi.wiley.com/10.1002/9781119992714.

[30] C. Carrillo, A. Obando Montaño, J. Cidrás, E. Díaz-Dorado, Review of power curve modelling for wind turbines, 5, Renew. Sustain. Energy Rev. 21 (2013) 572–581 [Online]. Available: http://linkinghub.elsevier.com/retrieve/pii/S1364032113000439.

[31] M. Lydia, S.S. Kumar, A.I. Selvakumar, G.E. Prem Kumar, A comprehensive review on wind turbine power curve modeling techniques, Renew. Sustain. Energy Rev. 30 (2014) 452–460 [Online]. Available: https://doi.org/10.1016/j.rser.2013.10.030.

[32] M.I. Blanco, The economics of wind energy, Renew. Sustain. Energy Rev. 13 (6–7) (2009) 1372–1382 [Online]. Available: http://linkinghub.elsevier.com/

retrieve/pii/S1364032108001299.
[33] WindEurope, Financing and Investment Trends, 2016 [Online]. Available: https://windeurope.org/about-wind/reports/financing-investment-trends-2016/.
[34] J. Aldersey-Williams, T. Rubert, Levelised cost of energy A theoretical justification and critical assessment, Energy Policy 124 (jan 2019) 169–179 [Online]. Available: https://linkinghub.elsevier.com/retrieve/pii/S0301421518306645.
[35] J. Olauson, P. Edström, J. Rydén, Wind turbine performance decline in Sweden, Wind Energy 8 (2017) [Online]. Available: http://doi.wiley.com/10.1002/we.2132.
[36] I. Staffell, R. Green, How does wind farm performance decline with age? Renew. Energy 66 (2014) 775–786 [Online]. Available: https://doi.org/10.1016/j.renene.2013.10.041.
[37] D. Vose, Risk Analysis: A Quantitative Guide, Wiley, 2008.
[38] D.J. Mundform, J. Schaffer, M.-J. Kim, D. Shaw, A. Thongteeraparp, P. Supawan, Number of replications required in Monte Carlo simulation studies: a synthesis of four studies, J. Mod. Appl. Stat. Methods 10 (1) (8 2011) [Online]. Available: http://digitalcommons.wayne.edu/cgi/viewcontent.cgi?article=1285context=jmasm.
[39] S.J. Watson, P. Kritharas, G.J. Hodgson, Wind speed variability across the UK between 1957 and 2011, January 2015, Wind Energy 18 (2013) 21–42 [Online]. Available: http://onlinelibrary.wiley.com/doi/10.1002/we.1679/full.
[40] P. Tavner, D.M. Greenwood, M.W.G. Whittle, R. Gindele, S. Faulstich, B. Hahn, Study of weather and location effects on wind turbine failure rates, Wind Energy 16 (2) (3 2013) 175–187 [Online]. Available: http://doi.wiley.com/10.1002/we.538.
[41] G. Wilson, D. McMillan, Assessing wind farm reliability using weather dependent failure rates, J. Phys. Conf. Ser. vol. 524 (6 2014) 012181 [Online]. Available: http://stacks.iop.org/1742-6596/524/i=1/a=012181?key=crossref.b8dc65677e053e3646aa421e267e73ed.
[42] M. Reder, J.J. Melero, Modelling the effects of environmental conditions on wind turbine failures, Wind Energy 5 (2018) [Online]. Available: http://doi.wiley.com/10.1002/we.2201.
[43] D. Cannon, D. Brayshaw, J. Methven, P. Coker, D. Lenaghan, Using reanalysis data to quantify extreme wind power generation statistics: a 33 year case study in Great Britain, Renew. Energy 75 (3 2015) 767–778 [Online]. Available: http://linkinghub.elsevier.com/retrieve/pii/S096014811400651X.
[44] I. Tobin, R. Vautard, I. Balog, F.-M. Bréon, S. Jerez, P.M. Ruti, F. Thais, M. Vrac, P. Yiou, Assessing climate change impacts on European wind energy from ENSEMBLES high-resolution climate projections, Clim. Change 128 (1–2) (1 2015) 99–112 [Online]. Available: http://link.springer.com/10.1007/s10584-014-1291-0.
[45] Megavind, Strategy for Extending the Useful Lifetime of a Wind Turbine, 2016.
[46] M. Schedat, T. Faber, A. Sivanesan, Structural Health Monitoring Concept to Predict the Remaining Lifetime of the Wind Turbine Structure, vol. 2016, Domestic Use of Energy, DUE, 2016.
[47] T.Q. Do, J.W. van de Lindt, H. Mahmoud, Fatigue life fragilities and performance-based design of wind turbine tower base connections, J. Struct. Eng. 141 (7) (2015) 04014183.
[48] A. Mehmanparast, J. Taylor, F. Brennan, I. Tavares, Experimental investigation of mechanical and fracture properties of offshore wind monopile weldments: SLIC interlaboratory test results, no. May, Fatigue Fract. Eng. Mater. Struct. (5 2018) 1–17 [Online]. Available: http://doi.wiley.com/10.1111/ffe.12850.
[49] D. Helm, Cost of Energy Review, 2017.